Confinement Effect on Interparticle Potential in Nematic Colloids

Mojca Vilfan,[1] Natan Osterman,[2] Martin Čopič,[1,2] Miha Ravnik,[2] Slobodan Žumer,[1,2] Jurij Kotar,[3] Dušan Babič,[2] and Igor Poberaj[2]

[1]*J. Stefan Institute, Jamova 39, SI-1000 Ljubljana, Slovenia*
[2]*Department of Physics, University of Ljubljana, Jadranska 19, SI-1000 Ljubljana, Slovenia*
[3]*Cavendish Laboratory, University of Cambridge, Cambridge CB3 0HE, United Kingdom*

(Received 9 August 2008; published 4 December 2008)

We studied the confinement effect on the interaction force in nematic liquid crystal colloids with spherical particles inducing planar anchoring. Using magneto-optical tweezers, we measured the spatial dependence of the quadrupolar structural interparticle force over 4 orders of magnitude. For small separations, the interparticle potential follows the power law, whereas for separations larger than the sample thickness, it decreases exponentially with the decay length proportional to the sample thickness. Experimental results are reproduced by using the Landau–de Gennes free-energy minimization approach.

DOI: 10.1103/PhysRevLett.101.237801 PACS numbers: 61.30.−v, 47.57.J−, 87.80.Cc

Interactions between colloidal particles have recently attracted considerable attention. In anisotropic liquids like nematic liquid crystals (NLC), a large number of phenomena, such as the formation of linear chains [1,2], hexagonal patterns [3,4], birefringent soft solids [5], nanocolloidal structures [6], and 2D colloidal crystals [7,8] have been observed. These effects are interesting for fundamental research and possible applications as photonic crystals, electronic paper and in microfluidics. These structures are stabilized by particle-induced elastic deformations in the LC director field, which lead to strong and highly anisotropic long-range interparticle forces. The distortions depend on the size, shape and surface properties of the particles. The director field around a sphere exhibits quadrupolar symmetry for tangential anchoring and dipolar or quadrupolar symmetry for homeotropic anchoring [9,10]. The elastic dipole can be transformed into an elastic quadrupole by an external field or surface confinement [11,12]. An analogy with electrostatics can be drawn where LC distortions correspond to charge multipoles and homeotropic anchoring to conducting plates. A mirror charges approach can be used and screening effects can thus be expected in colloidal systems.

Interactions in nematic colloids have been extensively investigated experimentally using optical microscopy and laser tweezers. Forces between two elastic dipoles were measured statically by determining the power of optical tweezers, which kept the beads at a given separation [13,14]. A combination of static and dynamic measurements gave the angular dependence of the force between two elastic quadrupoles [14]. Trajectories of released beads were used to dynamically study interactions between elastic quadrupoles and dipoles [15,16]. Unless very low laser power or a low-birefringent NLC is used [14], the local director configuration changes significantly due to the electric field of the laser light [17].

These reorientational effects can be completely avoided if magnetic field is used for manipulation of the particles instead of the focused laser light. First such measurements were performed by Poulin *et al.* [18], using ferrofluid droplets in NLC. Induced magnetic dipole moments drove the droplets apart. We implemented a similar idea but generated both attractive and repulsive forces between superparamagnetic particles in NLC by using either static or rotating magnetic field [19]. Static magnetic field was also used to analyze forces between homeotropic particles [20].

The interaction between two beads with tangential anchoring is of quadrupolar nature and follows a power law dependence $F \sim x^{-6}$ in a bulk nematic with x being the distance between the centers of the spheres [14,19,21]. In samples, confined by two flat surfaces, a difference in potential behavior is expected.

We show in this Letter by experiment and model that the interparticle potential at large separations no longer follows a power law, but—perhaps unexpectedly—decays exponentially. A decrease in the interparticle potential is observed at sphere separation comparable to and larger than the sample thickness. This is due to the boundary conditions and is in complete analogy with electrostatic interactions. The observed effect has to be taken into account when designing and studying tunable 2D colloidal crystals.

The potential between two spheres in the NLC was measured using combined magneto-optical tweezers [19]. The apparatus can operate in three different modes: (i) as optical tweezers; (ii) as magnetic tweezers generating repulsive force between two superparamagnetic particles, and (iii) as magnetic tweezers generating attractive force. The laser tweezers were used only for coarse initial positioning of the particles and were switched off during the measurements. Having no electric field and by keeping the

magnetic field low (~10 mT), we completely eliminated director reorientation due to external fields. The tweezers were built around an inverted optical microscope (Zeiss, Axiovert 200M, Achroplan 63/0.9W). For optical tweezers a Nd:YAG laser (1064 nm) was used and multiple traps were steered via acousto-optic deflectors (IntraAction) and a beam steering controller (Aresis, Tweez). Detection of the beads was done with a fast CMOS camera (PixeLINK) accompanied by a custom written particle tracking software enabling a position accuracy of ~10 nm.

Homogeneous magnetic field was generated by three orthogonal sets of Helmholtz coils regulated by a 6-channel computer-controlled current source. We used superparamagnetic beads, in which the induced magnetization was always parallel to the external magnetic field and proportional to the field magnitude for the fields used in the experiment. To obtain an attractive force between the beads without introducing angular momentum to the sample, we rotated the magnetic field in the sample plane in alternating clockwise and anticlockwise direction for 360° with a frequency of 400 Hz. The repulsive force was achieved when static magnetic field was perpendicular to the sample plane and cell walls prevented stacking.

The epoxy coated superparamagnetic spheres (Dynabeads, M-450 Epoxy, Dynalbiotech) with diameter $D = 4.4\ \mu$m [22] were mixed with NLC 4-*n*-pentyl-4'-cyanobiphenyl (5CB, Aldrich) at room temperature. By observing the spheres under a polarizing microscope we confirmed tangential anchoring at the surface. Homeotropic anchoring at the confining cell walls was achieved by using DMOAP silane-coated microscopic cover slides (Aldrich, 0.5% solution in water). When preparing the cell, a droplet of the NLC-spheres mixture was put on a microscopic cover slide and covered. LC elastic forces prevented sedimentation of the beads, which thus remained centered between the plates. Two beads were chosen and placed approx. 10 microns apart by optical tweezers (Fig. 1).

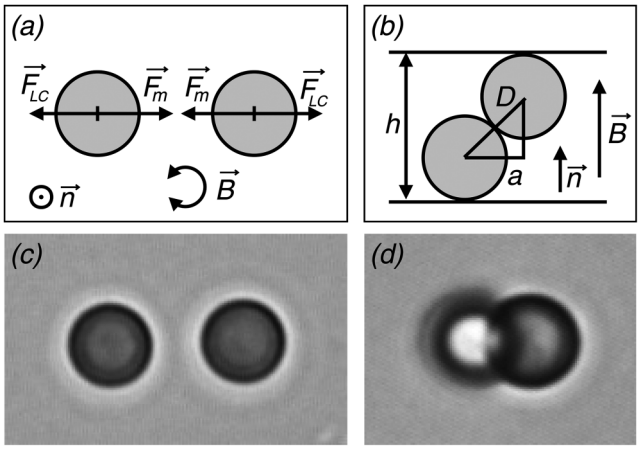

FIG. 1. (a) Schematic top view of the system. The LC-mediated force $\vec{F}_{\mathrm{LC}}$ was balanced by the magnetic force $\vec{F}_m$, achieved by a rotating magnetic field $\vec{B}$. Note the orientation of the nonperturbed director $\vec{n}$. (b) The sample thickness h was obtained by measuring the projection a. (c) Top view of the actual beads. (d) Two beads in contact that were used for determining the sample thickness. The difference in size is because only one bead is in the focal plane of the microscope. $D = 4.4\ \mu$m.

To measure the confinement effect on the interparticle interaction, cells with different thicknesses were prepared. The thickness h was determined after the cell was assembled by observing a pair of beads in contact under applied perpendicular magnetic field. The walls prevented the beads from stacking on top of each other [see Figs. 1(b) and 1(d)]. From the projection of the separation of spheres' centers a, h was obtained. The thickness of sample A was $h = 8.0(1 \pm 0.05)\ \mu$m, of sample B $h = 6.5(1 \pm 0.05)\ \mu$m, corresponding to $\sim 1.8D$ and $\sim 1.5D$, respectively.

We measured the interparticle force F by balancing the LC-mediated repulsive force and the calibrated attractive magnetic force. Magnetic force was set by electrical currents through the coils and the particle separation (for more see [19]). We stepwise reduced the electrical current, each time waiting for several minutes for the LC to fully relax and equilibrate, and measured the bead separation x. The force as a function of x was integrated in order to get the interparticle potential. The limiting value was set to zero for large x. The obtained potential $U(x)$ is shown in Fig. 2 as a log-log plot. The circles and squares are the measured data for sample A and B, respectively. The inset shows the interparticle force F as a function of separation x for sample A.

Multipole expansion approach predict power law behavior for force F and potential U [21] between two quadrupolar particles in bulk NLC: $F \propto (x/D)^{-6}$ and

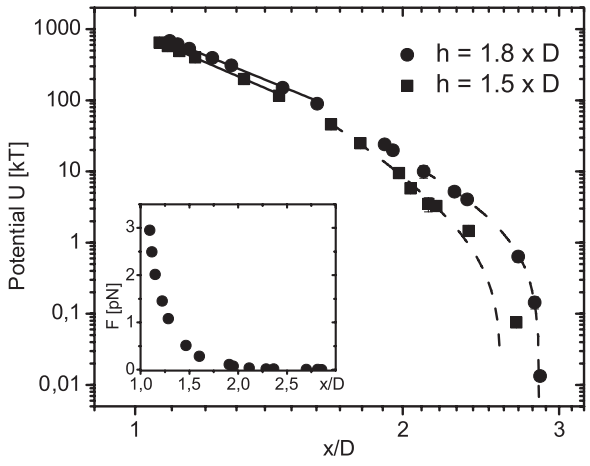

FIG. 2. Logarithmic plot of the interparticle potential as a function of normalized bead separation x/D for two cell thicknesses h. For small x/D, the data are fitted using power law function (solid lines) and for larger x/D, exponential function is used (dashed lines). The inset shows interparticle force F as a function of x/D for sample A. Experimental errors are of the size of the symbols.

$U \propto (x/D)^{-5}$ with the proportionality coefficients depending on the LC elastic constants and anchoring at the sphere surface.

We have shown previously [19] that the power law dependence is valid even for fairly small separations (down to $x \sim 1.1D$). Here we concentrate on the other limit of the power law validity. From Fig. 2 one clearly sees that the power law (solid line) fits the measured data only for a limited range of interparticle separations. The power law function $U = c_1/(x/D)^{\beta}$ can thus be fitted only for $x \lesssim 0.9h$, yielding the coefficients $\beta = 5.1(1 \pm 0.05)$ and $\beta = 5.4(1 \pm 0.10)$ for samples A and B, respectively. For particle separations comparable to or larger than the sample thickness, the influence of the confining walls is noticeable. For $x \gtrsim 1.2h$ the interparticle potential can be successfully fitted by an exponentially decaying function (dashed line):

$$U = c_2 \exp\left(-\frac{x}{\lambda}\right). \quad (1)$$

The obtained decay length λ is $\lambda = 1.41(1 \pm 0.10)\ \mu\text{m} = 0.18(1 \pm 0.15)h$ for sample A and $\lambda = 0.92(1 \pm 0.15)\ \mu\text{m} = 0.14(1 \pm 0.20)h$ for sample B.

The deviation from the power law dependence of the interparticle potential is governed by the confinement: for the interparticle separations comparable to or larger than sample thickness, the strong anchoring on the cell walls relatively reduces the effect of the beads on the director. The long range of the particle-induced deformation is thus suppressed (screened) and decays exponentially with cell thickness as a typical length scale. Exponential decay is expected also in the force profile, since the interparticle forces originate from director deformations. Similar screening effects were extensively studied in the defect annihilation processes [23,24].

The exponential interparticle interaction is also expected from an analogy with classical electrostatics [25,26]. Particles with tangential anchoring are analogous to electric quadrupoles and homeotropic confining surfaces to parallel conducting plates. The electrostatic potential of a quadrupole between two conducting plates can be written in the form of modified Bessel function $K_0(kx)$, which decays exponentially for large x [27]. The coefficient k is determined by the boundary conditions in the z direction: the solutions are proportional to $\sin(kz)$ and equal zero at the conducting plates. Using the analogy, assuming infinitely strong homeotropic anchoring on the cell walls and considering the symmetry of the director field around the immersed particle, the coefficient $k = 2\pi/h$ is obtained. The analogy with electrostatics thus gives a decay length $\lambda = 0.16h$, which is in excellent agreement with the experiment.

Numerical modeling of the interparticle potential was performed using Landau–de Gennes (LdG) free-energy minimization approach [28]. The LdG model uses invariants of the order parameter tensor Q_{ij} to construct phenomenologically the total free energy, which is then numerically minimized for given parameters and particle positions. Single elastic constant (L) free-energy volume density term $L(\partial Q_{ij}/\partial x_k)^2/2$ is used to model nematic elasticity, and "Landau" terms $A(Q_{ij}Q_{ji})/2 + B(Q_{ij}Q_{jk}Q_{ki})/3 + C(Q_{ij}Q_{ji})^2/4$ for the nematic order. Degenerate tangential anchoring at the particles' surface is modeled by the surface free energy density f_S [29]:

$$f_S = W(\tilde{Q}_{ij} - \tilde{Q}^{\perp}_{ij})^2, \quad (2)$$

where $\tilde{Q}_{ij} = Q_{ij} + S\delta_{ij}/2$, $\tilde{Q}^{\perp}_{ij} = (\delta_{ik} - \nu_i\nu_k)\tilde{Q}_{kl}(\delta_{lj} - \nu_l\nu_j)$, ν_k is the particle surface normal, S is the degree of the nematic order, and W the anchoring coefficient. Numerical minimization is performed explicitly on a cubic mesh by using finite differences. The material constants approximately correspond to 5CB and are together with the minimization method explained in [30]. Strong anchoring regime is chosen for particle surfaces ($W = 10^{-3}$ J/m^2) and infinite anchoring is assumed on cell walls. Particles with diameter $D = 1\ \mu$m are in the center of homeotropic cells with different cell thicknesses.

The calculated interparticle potential is plotted in Fig. 3. As the experiment, also the numerical model gives a combined power law and exponential behavior. Fitting the power law to the data for small x, we obtain the exponents $\beta = 4.5$, 5.0 and 6.2 for thicknesses $h = 2D$, $1.6D$, and $1.2D$, respectively. Note that in the thin sample, the window of the expected power-law behavior is fairly narrow as already at $x \sim 1.2D$ the exponential behavior prevails, making fit less reliable. Additionally, we comment that by assuming infinitely strong anchoring at the cell walls, the confinement effect is more pronounced as in experiments, resulting in higher values of the exponent β as well as shorter decay lengths λ. Using Eq. (1) to fit numerically

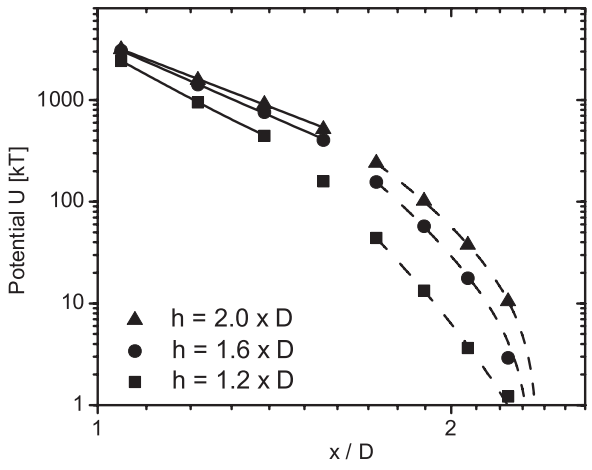

FIG. 3. Logarithmic plot of the numerically obtained interparticle potential as a function of normalized bead separation x/D for three different sample thicknesses h. For small x/D, the data are fitted using power law function (solid lines) and for larger x/D, exponential function is used (dashed lines).

obtained data for larger x yields the decay lengths: $0.11h$, $0.11h$, and $0.12h$ (for $h = 2D$, $1.6D$, and $1.2D$). We estimate the relative error of the numerically calculated power law exponents β and decay lengths λ to be 10%–20%.

Numerical results are in good qualitative agreement with experiments and electrostatic analogy. The crossover from the power law to the exponential behavior occurs at similar values of interparticle separations, approximately equal to the sample thickness. The exponential decay length is, consistent with the experiment, proportional to the sample thickness. The discrepancy may result from the assumption of infinitely strong anchoring on the cell walls and strong anchoring strength on the bead surface.

Experimental and numerical results show that the interaction between colloidal particles in a confined NLC is different from that in bulk. It decreases more rapidly than the power law, which means that the confinement reduces the potential range. This occurs because the cell walls induce strong alignment and when the separation between particles is comparable to or larger than the sample thickness, the LC director field between the spheres is less disturbed and the spheres interact as if they were further apart. Although similar behavior was observed in systems of nematic defect annihilation, this was the first actual study of the interparticle potential at larger separations, supported by numerical modeling of the system. We believe that such double-regime behavior and reduction of the long range of the potential has to be considered in designing new colloidal structures. Knowing the exact profile of the interparticle potential is essential for the optimization of the assembly processes in colloidal crystals. The crossover in the interaction potential is particularly relevant in colloidal crystals with tunable periodicity, where interparticle separations can be stretched beyond the power law validity regime.

To conclude, using magneto-optical tweezers we have observed crossover of the interparticle potential from power law to exponential decay at particle separations comparable to sample thickness. The decay length is found to be proportional to the sample thickness, causing a significant reduction of the potential. This confinement effect has to be considered when designing future colloidal structures.

The authors acknowledge support from ARRS P1-0099 and P1-0192 Programmes. M. V. acknowledges the support of NATO (Grant No. EAP.RIG.981424).

[1] P. Poulin, H. Stark, T. C. Lubensky, and D. A. Weitz, Science **275**, 1770 (1997).
[2] J.-C. Loudet, P. Barois, and P. Poulin, Nature (London) **407**, 611 (2000).
[3] I. I. Smalyukh *et al.*, Phys. Rev. Lett. **93**, 117801 (2004).
[4] A. B. Nych *et al.*, Phys. Rev. Lett. **98**, 057801 (2007).
[5] S. P. Meeker, W. C. K. Poon, J. Crain, and E. M. Terentjev, Phys. Rev. E **61**, R6083 (2000).
[6] O. Guzmán *et al.*, Phys. Rev. Lett. **91**, 235507 (2003).
[7] I. Muševič *et al.*, Science **313**, 954 (2006).
[8] M. Škarabot *et al.*, Phys. Rev. E **76**, 051406 (2007).
[9] H. Stark, Phys. Rep. **351**, 387 (2001).
[10] O. V. Kuksenok, R. W. Ruhwandl, S. V. Shiyanovskii, and E. M. Terentjev, Phys. Rev. E **54**, 5198 (1996).
[11] J. C. Loudet and P. Poulin, Phys. Rev. Lett. **87**, 165503 (2001).
[12] H. Stark, Phys. Rev. E **66**, 032701 (2002).
[13] M. Yada, J. Yamamoto, and H. Yokoyama, Phys. Rev. Lett. **92**, 185501 (2004).
[14] I. I. Smalyukh *et al.*, Appl. Phys. Lett. **86**, 021913 (2005); I. I. Smalyukh *et al.*, Phys. Rev. Lett. **95**, 157801 (2005); I. I. Smalyukh *et al.*, Proc. Natl. Acad. Sci. U.S.A. **103**, 18 048 (2006).
[15] M. Škarabot *et al.*, Phys. Rev. E **77**, 031705 (2008).
[16] U. Ognysta *et al.*, Phys. Rev. Lett. **100**, 217803 (2008).
[17] I. Muševič *et al.*, Phys. Rev. Lett. **93**, 187801 (2004).
[18] P. Poulin, V. Cabuil, and D. A. Weitz, Phys. Rev. Lett. **79**, 4862 (1997).
[19] J. Kotar *et al.*, Phys. Rev. Lett. **96**, 207801 (2006).
[20] C. M. Noël *et al.*, Phys. Rev. Lett. **96**, 217801 (2006).
[21] R. W. Ruhwandl and E. M. Terentjev, Phys. Rev. E **55**, 2958 (1997).
[22] G. Fonnum *et al.*, J. Magn. Magn. Mater. **293**, 41 (2005).
[23] A. Bogi, P. Martinot-Lagarde, I. Dozov, and M. Nobili, Phys. Rev. Lett. **89**, 225501 (2002).
[24] D. Pires, J.-B. Fleury, and Y. Galerne, Phys. Rev. Lett. **98**, 247801 (2007).
[25] T. C. Lubensky, D. Pettey, N. Currier, and H. Stark, Phys. Rev. E **57**, 610 (1998).
[26] V. M. Pergamenshchik and V. O. Uzunova, Eur. Phys. J. E **23**, 161 (2007).
[27] J. D. Jackson, *Classical Electrodynamics* (John Wiley & Sons, New York, 1975), 2nd ed.
[28] P. G. de Gennes and J. Prost, *The Physics of Liquid Crystals* (Oxford Science, Oxford, 1993), 2nd ed.
[29] J. B. Fournier and P. Galatola, Europhys. Lett. **72**, 403 (2005).
[30] M. Ravnik *et al.*, Phys. Rev. Lett. **99**, 247801 (2007).